ACS OMEGA

http://pubs.acs.org/journal/acsodf

Article

Enhancement of Isotropic Heat Dissipation of Polymer Composites by Using Ternary Filler Systems Consisting of Boron Nitride Nanotubes, h-BN, and Al_2O_3

Arni Gesselle M. Pornea, Ki-In Choi, Jung-Hwan Jung, Zahid Hanif, Cheolwoo Kwak, and Jaewoo Kim*

Cite This: *ACS Omega* 2023, 8, 24454−24466

Read Online

ACCESS | Metrics & More | Article Recommendations | Supporting Information

ABSTRACT: In this research article, a poly(dimethylsiloxane) (PDMS)-based composite was postulated adapting an interactive ternary filler system consisting of Al_2O_3, hexagonal boron nitride (h-BN), and boron nitride nanotubes (BNNT) to construct a continuous three-dimensional (3D) structure for thermal attenuation. Al_2O_3 was imposed as a main filler, while h-BN and BNNT were assimilated to form interconnected heat conduction pathways for effective thermal dissipation. The structured framework articulates a profound improvement in isotropic thermal conductivity considering both axial and radial heat dissipation. The presence of h-BN entails uniform heat distribution in a planar mode, eliminating the occurrence of hotspots, while BNNT constructed a connecting phonon pathway in various directions, which insinuates effective overall thermal transport. The generated ternary filler composites attained an isotropic ratio of 1.35 and a thermal conductivity of 7.50 W/mK, which is a 36-fold (~3650%) increase compared to neat PDMS resin and almost 3-fold (~297%) that of the Al_2O_3 unary filler composite and ~53% that of its binary counterpart, partaking interfacial thermal gaps of ~36.15 and ~62.24% on practical heating performance relative to its counterparts. Moreover, the incorporation of BNNT on a traditional spherical and planar filler offers an advantage not only in thermal conductivity but also in thermal and structural stability. Improvement in thermal stability is stipulated due to a melting point (T_m) shift of ~11 °C upon the assimilation of BNNT. Mechanical permeance reinforcement was also observed with the presence of BNNT, showcasing a 31.5% increase in tensile strength and a 53% increase in Young's modulus relative to the singular filler composite. This exploration administers a new insight into heat dissipation phenomena in polymeric composites and proposes a simple approach to their design and assembly.

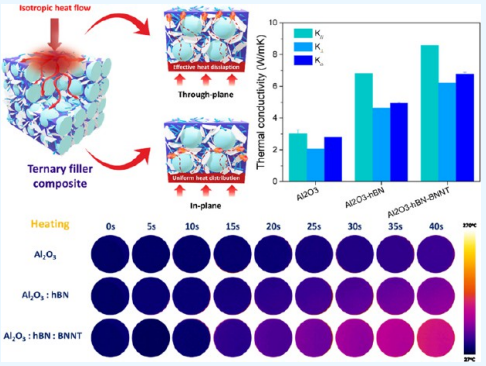

1. INTRODUCTION

As we approach the fifth-generation (5G) network era, current electronic devices adapt alongside this progressing technology.[1−4] However, the advances toward high speed, integrability, and portability in these devices result in the densification of the integrated circuit (IC) distribution, resulting in thermal challenges. Much attention has been invested in heat control advancement to resolve the thermal throttling effect on these electronic devices and systems, since the accumulated heat in these microelectronics hampers their performance, reliability, and life span. To eradicate the heat build-up from these devices, heat-conducting media such as TIM with high thermal conductivity must be implemented to provide a resolution to the dilemma on these devices.[5,6]

The overall thermal ejection property of TIM is highly reliant on the geometrical stature of the fillers and their corresponding intrinsic properties. Several attempts have been expounded to elevate the thermal conductivity of polymer-based TIM through the introduction of conductive fillers and additives in different shapes and sizes such as carbonaceous materials, silicon nitride, boron nitride, metals, etc.[7−13] TIM is commonly established through the straightforward process of direct integration of a conductive filler and a polymeric matrix to attain high thermal conduction. In this accord, numerous combinations of fillers with varying geometrical configurations and arrangements were enacted to fortify the overall thermal conductance of TIM. Spatially oriented multiscale fillers are proven to establish continuous filler networks to accentuate thermal conduction.[14] Hence, these proclaimed approaches post limitations in terms of the heightened electrical conductivity of the composite, which can hamper the IC's longevity due to the utilization of carbonaceous materials and metals. On the contrary, ceramic-based fillers such as aluminum oxide, silicon nitride, silicon oxide, and boron nitride have been opted for as indispensable options.[6,15,16]

Received: April 3, 2023
Accepted: June 19, 2023
Published: June 29, 2023

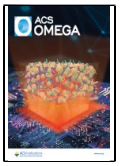

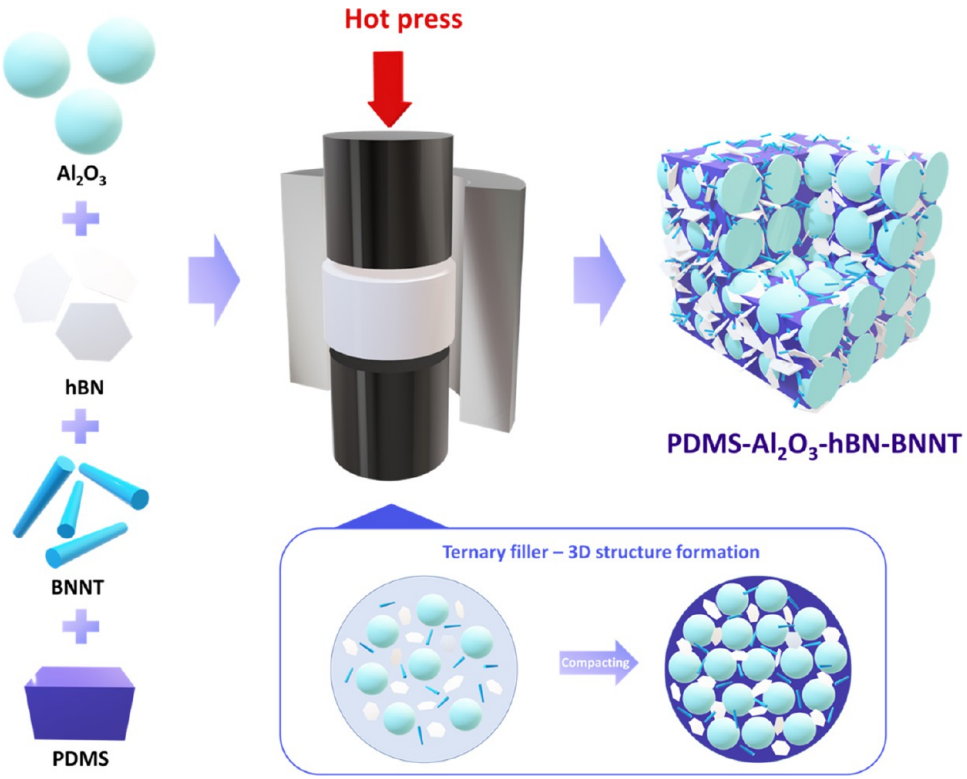

Figure 1. Schematic representation of the fabrication strategy of the ternary filler composite.

h-BN, an analogue of layered graphite, acts as a promising thermal transport-inducing filler mainly due to its high thermal conductivity, which approaches ∼300 W/mK, with other advantageous attributes such as high elastic modulus, high electrical insulation, relatively low dielectric coefficient, and low density, which are highly appreciated in numerous fields.[15,17−22] However, due to the planar nature of h-BN, most of the h-BN-based composites showed an anisotropic characteristic, producing superior in-plane and inferior through-plane thermal conduction behaviors. To instigate an effective heat dissipation behavior, one should thoroughly consider both in-plane and through-plane thermal conductivities. Through-plane orientation directly influences the heat transport outside the system while maintaining a stable device temperature, on the other hand, in-plane direction helps to ease the occurrence of concentrated heat or hotspots. Therefore, both in-plane and through-plane thermal conductivities are of equal importance for the resolution of heat accumulation on electronic devices. Notably, a distinct number of research groups have demonstrated several strategies to insinuate heat conduction pathways for the enhancement of h-BN-based thermal conduction in the through-plane direction by filler orientation modification.[23,24] Wang et al. fabricated a self-assembled three-dimensional (3D) h-BN composite with 30 wt % filler content obtaining a thermal conductivity of 1.28 W/mK.[25] Likewise, Park et al. developed a shear-induced strategy to prepare an oriented h-BN arrangement; the conveyed approach showcased an in-plane thermal conductivity of 10.1 W/mK, while through-plane thermal conductivity reached 0.28 W/mK.[26] Relatively, vertically oriented h-BN was also forged to exhibit improved through-plane thermal conductivity; however, this strategy culminated a decreased in-plane thermal conductivity not to mention its procedural difficulty.[27−29] Additionally, Fu et al. reported a ternary filler system with PA6 as the main filler assisted by two planar supporting filler additives (GO and h-BN) to prompt a continuous filler network; hence, the proposed strategy still establishes an inferior vertical thermal conductivity.[30] Despite these advancements, most of these composites still project a large gap between in-plane and through-plane thermal conductivity, which impedes the TIM overall heat ejection capability.[31]

Deliberate attempts have been adapted for the development of highly thermally conductive composites for effective heat ejection on electronic devices through multidimensional filler structural design tunning. In this research article, we presented a systematic strategy for a filler's geometrical arrangement, thereby improving the overall performance of the stipulated composite in thermal and mechanical aspects. Given the liberty to select incorporating materials to satisfy the utilization requirements, multimodal fillers containing Al_2O_3 (3D), h-BN (two-dimensional (2D)), and BNNT (one-dimensional (1D)) were chosen in the pursuit to construct a highly conductive composite. It is postulated that the assimilation of the multidimensional fillers forms a 3D structural arrangement and is expected to form an accentuated heat dissipation network,[32,33] which (1) eradicates the occurrence of hotspots, (2) insinuates effective overall thermal transport, and (3) abates phonon scattering. The composite was based on poly(dimethylsiloxane) (PDMS), a frequently utilized polymer due to its permanency, viability, and versatility, which is vastly favored in various fields.[34,35] Al_2O_3 was imposed as a based filler, while h-BN and BNNT were assimilated to form an interconnected heat conduction pathway for effective thermal transport.[36] The Al_2O_3 particles act as a node in the hybrid filler design, while boron nitride serves as a connecting channel for phonons to flow, which suggests effective thermal transport. Traditionally, h-BN is intercalated onto the Al_2O_3 surface,

https://doi.org/10.1021/acsomega.3c02246
ACS Omega 2023, 8, 24454−24466

trailing its spherical shape, which is highly beneficial for hotspot elimination due to the planar nature of h-BN.[37] On the other hand, the introduction of BNNT reinforces filler contact points, augmenting the isotropic phonon transport and thereby rectifying the in-plane thermal conductivity dominance of h-BN.[38] As presumed, one-dimensional geometrical fillers offer a significant thermal conductivity increase compared to other filler shapes, as they can intercalate with other fillers due to their high aspect ratio, which promotes long conductive heat pathways.[39] BNNT acted as a bridge to boost the phonon transport in various directions, thereby improving the isotropic heat transfer.[40] Besides the geometrical and structural contribution of boron nitride, the similarity in elemental characteristics of h-BN and BNNT can prompt an improvement in phonon conduction due to their matching phonon acoustic property, thus encouraging seamless phonon transport and reduction of phonon scattering.[31,15] To the best of our knowledge, this is the first attempt to devise a ternary hybrid composite system using Al_2O_3, h-BN, and BNNT to enact isotropic heat pathways and subdue phonon scattering for effective overall thermal transport. Hence, this investigation provides new insights into heat dissipation phenomena in polymeric composite systems and suggests a systematic technique for their design and structuralization with a relatively simple approach.

2. EXPERIMENTAL SECTION

2.1. Materials. Al_2O_3 microparticles (~90 μm) were purchased from Denka Korea. h-BN (10 μm, purity: 99%) was acquired from Unitech Corporation. The BNNT powder (diameter: 30−50 nm, length: ~10 μm, purity: >80%) was synthesized by using a thermochemical reaction of boron powder with nitrogenous gases.[26,27] The purity of BNNT indicates the fraction of nanotubes in weight, while the remainder is h-BN nanoparticles and nanoflakes. PDMS resin and curing agents (Sylgard 184A and Sylgard 184B) were provided by Sewang Hightech Silicone.

2.2. Preparation of the Ternary Filler Composite. As presented in a schematic representation in Figure 1, the ternary filler system was processed by simply combining PDMS with different fillers through consecutive mechanical mixing with the aid of a phase mixer. Comparative filler systems were prepared to affirm the isotropic thermal conduction superiority of the ternary filler system (PDMS-Al_2O_3, PDMS-Al_2O_3-h-BN, and PDMS-Al_2O_3-h-BN-BNNT); a single filler system was prepared by mixing 90 wt % Al_2O_3 particles, while the binary and ternary filler systems were assembled by changing 13.50 wt % of the filler content with boron nitride derivatives following the same fractional concentration. Moreover, the overall filler content of the ternary composite system was varied at 90, 80, and 70 wt %, to accentuate the contribution of the filler concentration while maintaining the boron nitride derivative ratio constant. The fractional concentrations of the boron nitride derivatives were also varied to construe the synergistic and geometrical influence of the multidimensional filler additives (h-BN/BNNT = 1:0, 2:1, 1:1, 1:2, 0:1). Initially, a mixture of PDMS resin part A (Sylgard 184A) was diluted with a thinner (5% of the overall weight), and then BNNT were introduced followed by mechanical paste mixing. Subsequent incorporation of the remaining filler was accomplished with the same approach in an orderly manner combining BNNT and h-BN, followed by Al_2O_3, and a homogeneously mixed paste was obtained after the process. Afterward, PDMS resin part B (Sylgard 184B) was then fused with the acquired paste mixture and subjected to mechanical mixing again to ensure its homogeneous distribution. The final paste mixture was then loaded onto a metallic mold and underwent hot-pressed curring treatment. The same procedure was also applied in the preparation of the unary and binary filler composites.

2.3. Characterization. The morphological and structural attributes of the prepared composites were observed through a field emission scanning electron microscope (FESEM, CX-200 COXEM), and the samples were prepared through liquid nitrogen freezing followed by cross-sectional fracture of the composite. Fourier transform infrared (FTIR, PerkinElmer Spectrum Two FTIR-ATR) spectra were collected with a 4 cm^{-1} resolution and an accumulation of 32 scans with the range of 500−4000 cm^{-1}. The thermal stability of the generated composites was observed using a thermogravimetric analyzer (TGA), which was administered at a heating rate of 10 °C/min in the 100−800 °C thermal range under a nitrogen atmosphere. The differential scanning calorimetry (DSC, Labsys Evo TG-DTA) was used to check the glass transition temperature (T_g) of the generated samples. The densities, thermal diffusivities, and specific heat of the fabricated composites were determined by laser flash analysis (LFA, Netzsch Instruments Co., LFA-467). The through-plane thermal conductivity ($k_\perp$, W/mK) was calculated by $k_\perp = \rho \times C_p \times \alpha$, where ρ (g/cm) stands for density, Cp (J/gK) signifies specific heat, and α (mm^2/s) implies thermal diffusivity. Hence, since our aim is to demonstrate effective overall thermal conductivity connotating heat dissipation through in-plane ($k_{//}$) and through-plane ($k_\perp$) directions, we chose isotropic thermal conductivity (k_o) measurement using a thermal analyzer (Hot-Disk thermal analyzer, TPS500S) to represent the thermal dissipation performance of the fabricated ternary filler composites. $k_{//}$ and $k_\perp$ measurements were also expounded at the beginning of the thermal conduction discussion to enunciate the relationship of the filler orientation to the thermal performance of the composites. The heat dissipation attribute in the practical applications of the composites was assessed by a homemade heating device to mimic the heating (as well as cooling in an ambient environment) properties of an actual electronic device system; the heat propagation was then observed by an infrared camera (IR-camera, COX CX-Series). The compression modulus of the prepared samples was acquired using a universal testing machine (UTM, Withlab Co., Ltd.).

3. RESULTS AND DISCUSSION

3.1. Morphological Attributes of the Ternary Filler Composite. The technique adopted here to stimulate thermal conductivity is structural augmentation through a combination of various multidimensional fillers such as Al_2O_3 (3D), BNNT (1D), and h-BN (2D) to devise an improved filler-to-filler interaction. The thermal conductivity of a polymeric composite highly relies on the inherent properties of the polymer and fillers; hence, the geometrical orientation of these fillers post a substantial influence on thermal conductivity.[41,42] Therefore, the morphological attributes of the fabricated composites were thoroughly observed to articulate the interaction between the fillers and to retaliate its relation with the thermal conductivity performance. Al_2O_3, h-BN, and BNNT are utilized as unary, secondary, and ternary fillers, respectively, to prepare TIM; the SEM illustration of each filler is presented in Figure S1 to display their geometrical attributes.

https://doi.org/10.1021/acsomega.3c02246
ACS Omega 2023, 8, 24454−24466

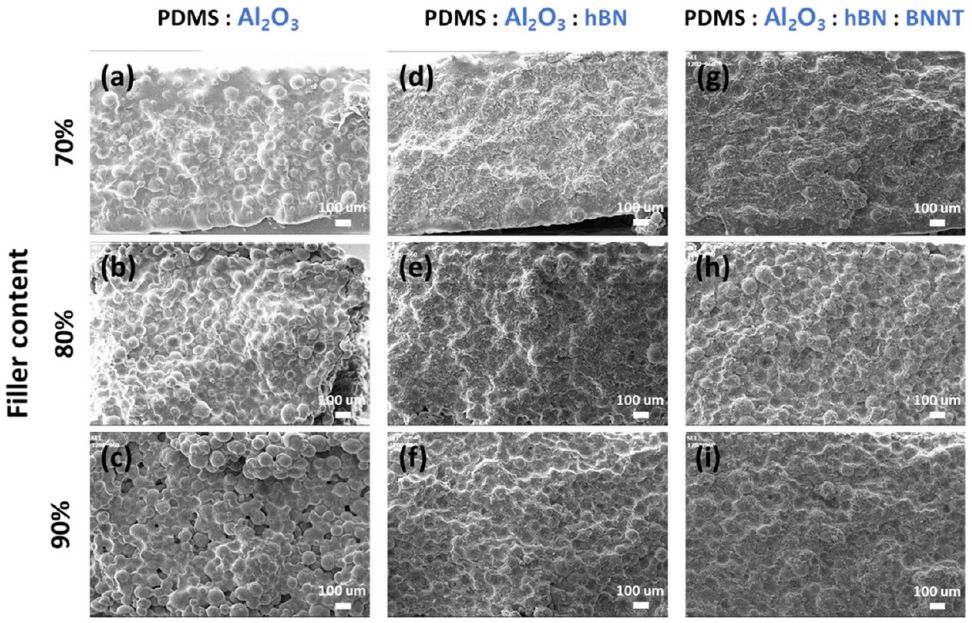

Figure 2. SEM images of the fabricated primary, secondary, and ternary filler systems with varied filler contents. (a–c) PDMS-Al_2O_3, (d–f) PDMS-Al_2O_3-h-BN, and (g–i) PDMS-Al_2O_3-h-BN-BNNT.

SEM images were also accomplished and are presented in Figure 2a–i to attest and demonstrate the architectural attributes of different composite systems with varied filler compositions and concentrations. The structural aspects of the composites with different filler contents were observed, where the neat Al_2O_3 sample projected a traditional spherical packing feature. On the other hand, the introduction of h-BN sheets illustrated a planar arrangement onto the Al_2O_3 interface, thereby insinuating contact points between particles, projecting better filler stacking due to the ability of h-BN to permeate the voids between the Al_2O_3 particles. The introduction of BNNT into the sphere-plate filler system presents an opportunity to occupy the void spaces that h-BN cannot fill due to its geometrical limitations. Across all of the concentration conditions, h-BN sheets can easily be discerned, while BNNT can only be observed on higher magnification, as presented in Figure S2. This can be ascribed to the difference in geometrical attributes of h-BN and BNNT, where the apparent visual dominance of h-BN can be correlated to its larger interfacial area. Moreover, the tubular structure and nanosize diameter of BNNT make it susceptible to polymeric wrapping, which makes it imperceivable.

With respect to the overall structural framework of the composites with different h-BN and BNNT ratios as presented in Figures 3a–o and S3, there is no apparent distinction in the arrangement of the Al_2O_3 particles. Due to the geometry and scale of h-BN and BNNT, the disparity can only be observed at the micro/nanometric level. Hence, the assimilation of these multidimensional particles was intended to articulate phonon pathways for effective heat dissipation owing to the structural and percolation contributions of h-BN and BNNT. The intercalation between h-BN plates and BNNT can be discerned on all the ternary filler composites relative to the proportion condition.

3.2. Chemical and Physical Characterization. Illustrated in Figure 4a are the FTIR spectra of the fabricated PDMS-based composites. The plain PDMS polymer showed peaks at 2961 and 1080 cm^{-1}, which depicts the stretching vibrations of CH_3 and Si–O–Si, respectively, while peaks at 1260 and 788 cm^{-1} are associated with the symmetric deformation of the CH_3 group and stretching oscillation of Si–O, respectively.[43] The peak at 560 cm^{-1} on the primary composite corresponds to the introduction of the Al_2O_3 base filler.[44] Peaks can be discerned at 1367 and 804 cm^{-1} upon the introduction of boron nitride derivatives; these peaks were allocated to B–N stretching vibrations and B–N–B bending vibrations, respectively.[45] All discerned polymeric peaks can be realized on all prepared composites analogous to their confining materials.

The thermal attributes of the generated ternary composite and its derivatives were observed through TGA curves from the 50 to 800 °C range, as presented in Figure 4b. The samples were measured under nitrogen gas to affirm their thermal stability. All of the configured samples illustrate one thermal degradation step; the pristine PDMS started to degrade at 350 °C and acquired the lowest residual amount among all of the samples, suggesting its polymeric properties.[46] On the other hand, upon introduction of the fillers, an apparent elevation in thermal stability is realized, which can be constituted by their intrinsic thermal characteristics. More importantly, the thermal stability of BNNT-integrated composites was much increased compared to other samples. It can be observed that the temperature for the disintegration of the polymeric chains of the sample with BNNT reached ∼550 °C, while both Al_2O_3 and Al_2O_3-h-BN filler systems began to deteriorate at ∼450 °C. This was also confirmed by the DSC data in Figure 5a, affirming the relationship between the crystallinity and multidimensional filler loading of the fabricated samples. The melting point T_m of the BNNT-assimilated sample projected an increasing trend relative to the ones with other filler systems, showcasing its contribution to the composite's thermal stability,[40] which can be correlated to BNNT's distinct geometrical dominance and potent intrinsic permanence.

Considering the sensible concept of the developed heat-dissipating composites in practical application, the scrutinization of mechanical performance is imperative. TIM usually

https://doi.org/10.1021/acsomega.3c02246
ACS Omega 2023, 8, 24454–24466

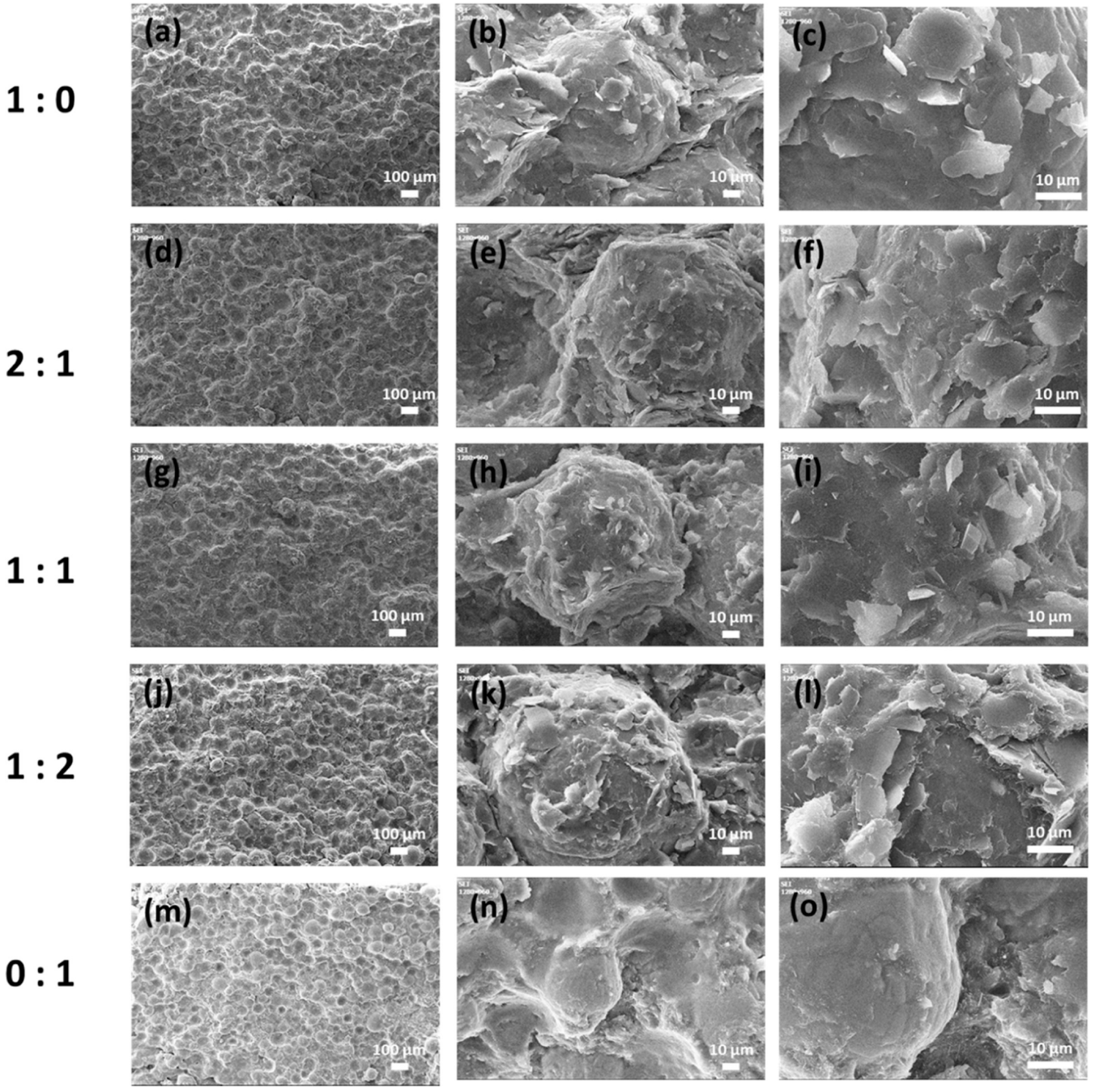

Figure 3. SEM images of the fabricated ternary filler composite with different ratios of h-BN and BNNT (h-BN/BNNT): (a–c) 1:0, (d–f) 2:1, (g–i) 1:1, (j–l) 1:2, and (m–o) 0:1.

requires a different mode of assembly and application, which demands good flexibility and excellent compressive property. To precisely construe the filler influence on the mechanical performance of the formed composite, we thereby expounded a tensile test on the crafted ternary composite and its corresponding derivatives, as shown in Figure 5b and Table 1. The BNNT-incorporated composite established a tensile strength of 6.22 MPa, whereas the Al_2O_3-h-BN and Al_2O_3 filler-added systems demonstrated tensile strengths of 5.09 and 4.73 MPa, respectively, while maintaining the elongation property, which reflects the effective filler network construction contribution of BNNT. In addition, Young's modulus for the BNNT-incorporated system was increased by ∼21 and ∼53% with respect to Al_2O_3-h-BN and Al_2O_3 filler systems. The mechanical performance improvement can be associated with the inclusion of boron nitride derivatives, mainly BNNT due to their tubular form, which tends to stipulate durability and potent structural flexibility and also provides leverage toward thermal regulation application.

3.3. Thermal Conductivity Performance of the Ternary Filler Composite. Numerous techniques were implemented to develop the isotropic thermal conductivity of polymeric composites. Conversely, the relative thermal conductivity of these composites tends to favor one heat route over the other, which depends on the inherent attributes of the filler materials. To instigate an efficient heat transport

https://doi.org/10.1021/acsomega.3c02246
ACS Omega 2023, 8, 24454−24466

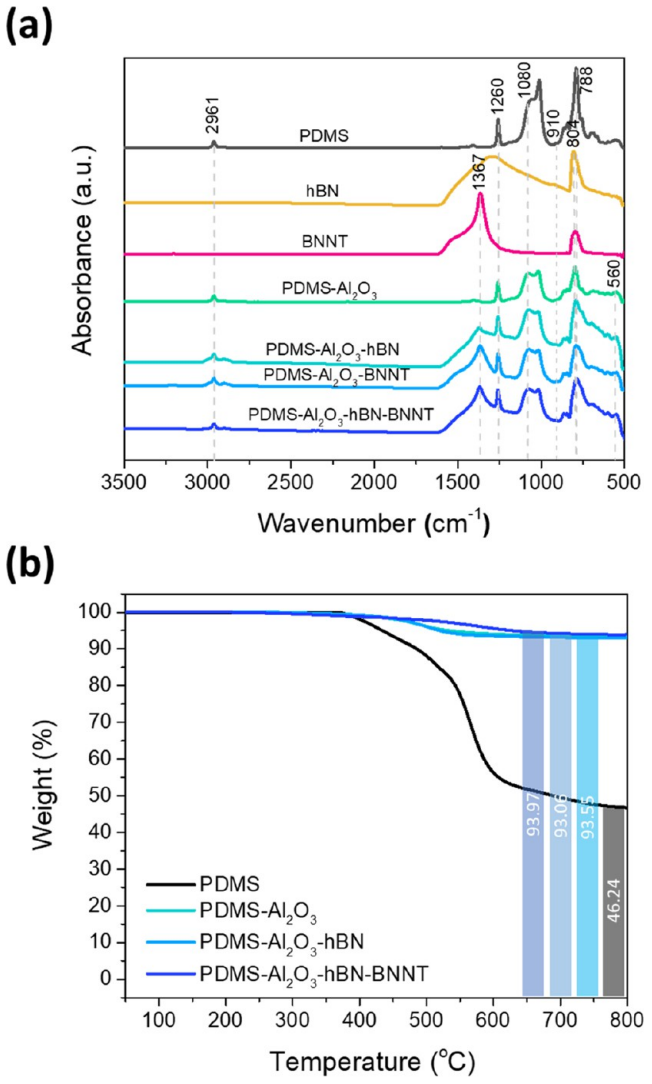

Figure 4. Ternary filler composite and its corresponding derivatives: (a) FTIR spectra and (b) TGA.

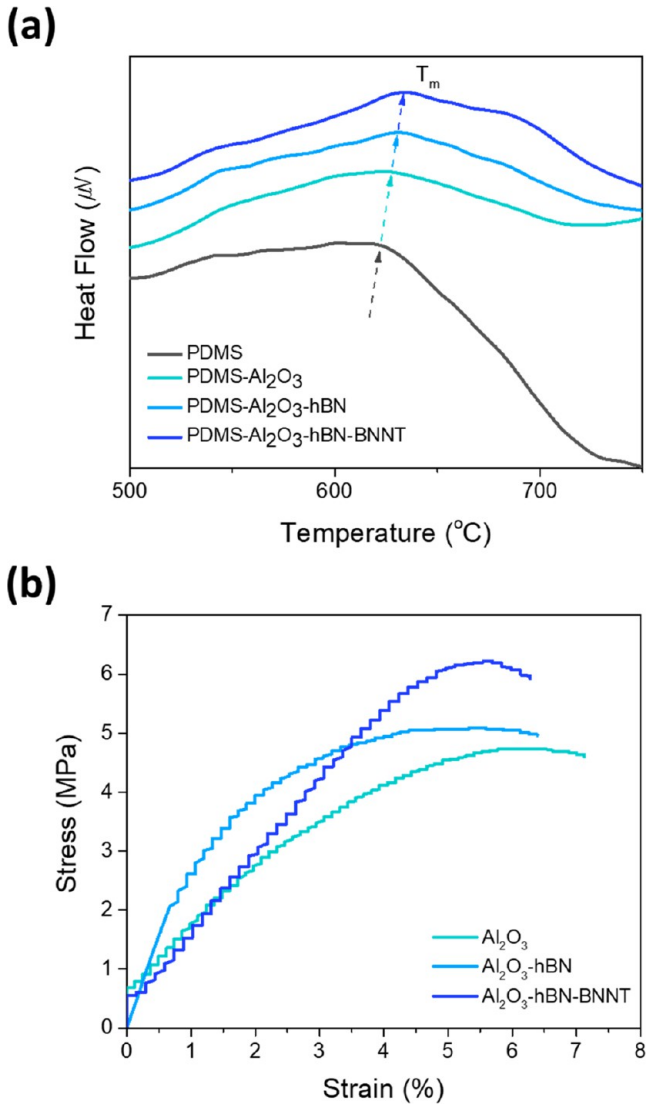

Figure 5. Ternary filler composite and its corresponding derivatives: (a) DSC and (b) stress/strain profiles.

mechanism, one should systematically consider both $k_{\perp}$ and $k_{//}$, given that $k_{\perp}$ orientation directly influences the heat dissipation of the system, while the $k_{//}$ direction helps to ease the occurrence of concentrated heat or hotspots. It has been previously explored that the incorporation of particles of different shapes and sizes can elevate the overall thermal conductivity, and the effectiveness of heat dissipation is highly reliant on the filler's intrinsic thermal conductivity, fractional loading, filler geometry, dispersion, and structural orientation.[5,40,47] In this regard, a ternary filler system using the PDMS composite was articulated, as illustrated in Figure S4; Al_2O_3 was utilized as a base filler while h-BN and BNNT were integrated to systemize an organized heat conduction pathway for multidirectional heat transport.

Illustrated in Figure 6a are the $k_{//}$, $k_{\perp}$, and k_o thermal conductivities of the prepared composites. It can be discerned that all samples follow the same trend on the different thermal conductivity modes of measurement, with $k_{//}$ thermal conductivity attaining the highest measurement. The singular filler system attained the lowest thermal conductivity due to minimal contact points and a heat conduction pathway between the Al_2O_3 particles, as shown in the SEM images. The binary composite system on the other hand showcased a steep thermal conductivity improvement compared to the Al_2O_3 unary composite, while the ternary composite posted a heightened thermal conductivity augmentation in accordance with its counterparts, demonstrating the thermal contact enhancement of the articulated ternary system. The same trend can also be noticed in the thermal diffusivity of the measured samples, having 1.1 mm^2/s for the unary filler system followed by 2.512 mm^2/s for the binary system, while the ternary system reached 2.650 mm^2/s. The difference in the thermal diffusivities of the devised systems promulgates the construction of the thermal conduction pathways and the abatement of the occurrence of phonon scattering.

Table 1. Stress and Strain Values of the Fabricated Composites

sample	stress (MPa)	strain (%)	Young's modulus
Al_2O_3	4.73	6.51	72.66
Al_2O_3-h-BN	5.09	5.59	91.06
Al_2O_3-h-BN-BNNT	6.22	5.69	109.31

To validate the filler structural orientation relationship with the heat dissipation direction, the isotropic ratio between $k_{//}$

https://doi.org/10.1021/acsomega.3c02246
ACS Omega 2023, 8, 24454−24466

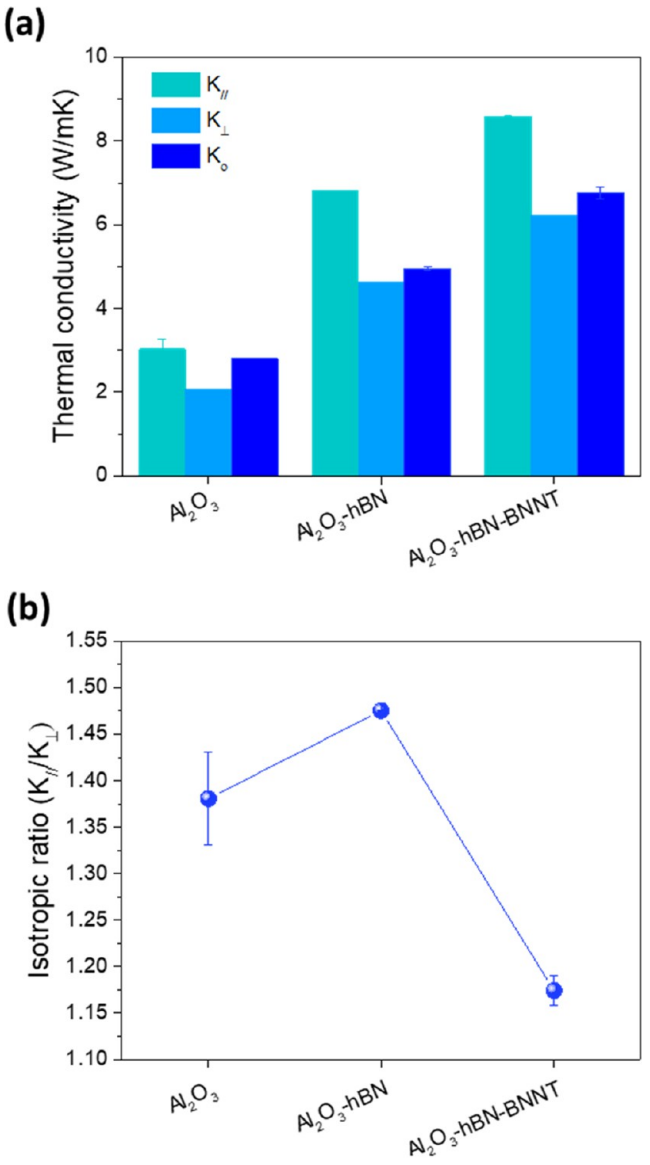

Figure 6. (a) Different thermal conductivity ($k_{//}$, $k_{\perp}$ and k_o) measurements of the produced hybrid composites with 90% filler concentration and its corresponding (b) isotropic ratio ($k_{//}/k_{\perp}$).

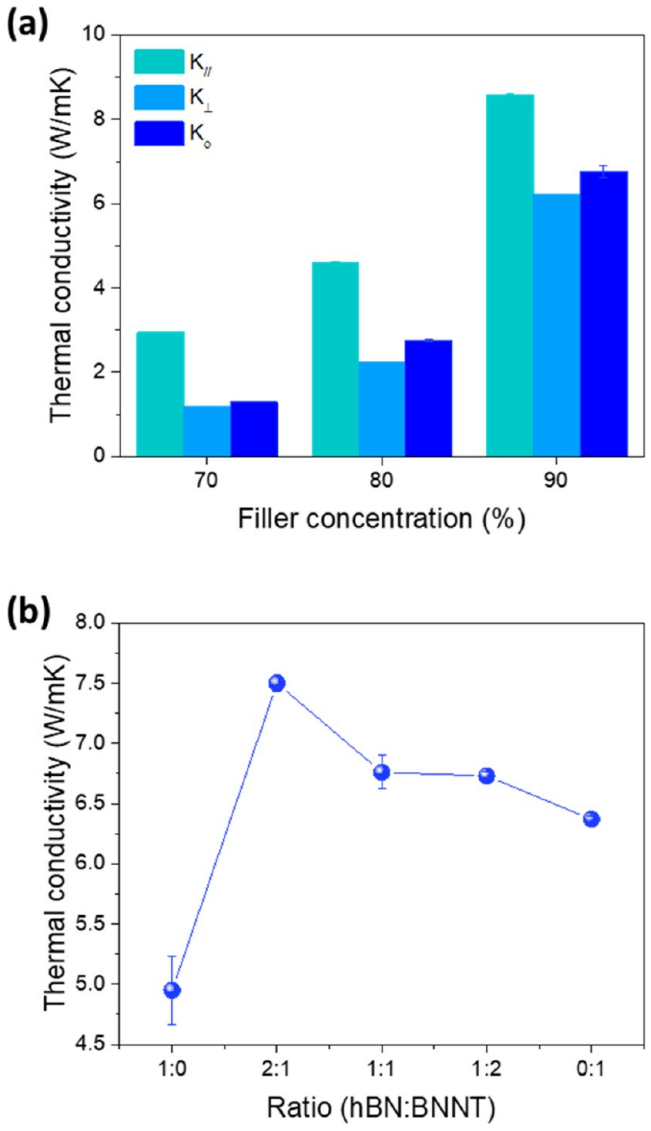

Figure 7. (a) Different thermal conductivity ($k_{//}$, $k_{\perp}$, and k_o) measurements of the ternary filler composite with varied filler concentrations. (b) Isotrophic thermal conductivity measurement of the ternary filler composite with diverse ratios of h-BN and BNNT.

and $k_{\perp}$ was analyzed, as shown in Figure 6b. Even though the introduction of h-BN facilitated an incremented contribution to thermal conductivity, an increase in the gap between $k_{//}$ and $k_{\perp}$ can be observed on the binary filler composite, which is analogous with the common h-BN performance due to its planar geometry. On the other hand, the introduction of BNNT minimized the gap between $k_{//}$ and $k_{\perp}$, posting the lowest gap among all of the samples. This can be linked to the geometrical influence of the filler additives on the structural arrangement and interaction of the fillers, which conjectures the isotropic thermal conductivity. Hence, this affirms the contribution of the BNNT to dissipate heat in a multidirectional manner. Different filler concentration conditions were prepared to assert the heat conduction dominance of the proposed ternary filler system, as shown in Figure 7a. Pristine PDMS attained an isotropic thermal conductivity of ~0.20 W/mK, which follows the traditional low thermal conductivity of polymers, which can be correlated to its disordered crystalline structure and extrinsic scattering.[15] The thermal conductivity profile of the prepared composites was comprehensively analyzed through different thermal conductivity measurement modes relative to the elevation of the filler concentration, where all samples projected a sharp increase in thermal conductivity upon filler content escalation. An elevation in the heat conduction on the ternary composites was coherently observed throughout all of the various filler weight fractions, signifying the filler influence on the overall thermal conductivity of the composite. The ternary filler (Al_2O_3-h-BN-BNNT) composite acquired an isotropic thermal conductivity of 6.76 W/mK at 90 wt % total filler content, which is 1.41-fold that of the binary filler (Al_2O_3-h-BN) composite. Since we aim to demonstrate effective isotropic thermal transport considering the composite's practical application, we choose to present consecutive measurements in isotropic thermal conductivity.

It is established that thermal conductivity is highly influenced by the constructed polymeric matrix and interconnected filler networks.[48] Therefore, discrete loading

https://doi.org/10.1021/acsomega.3c02246
ACS Omega 2023, 8, 24454−24466

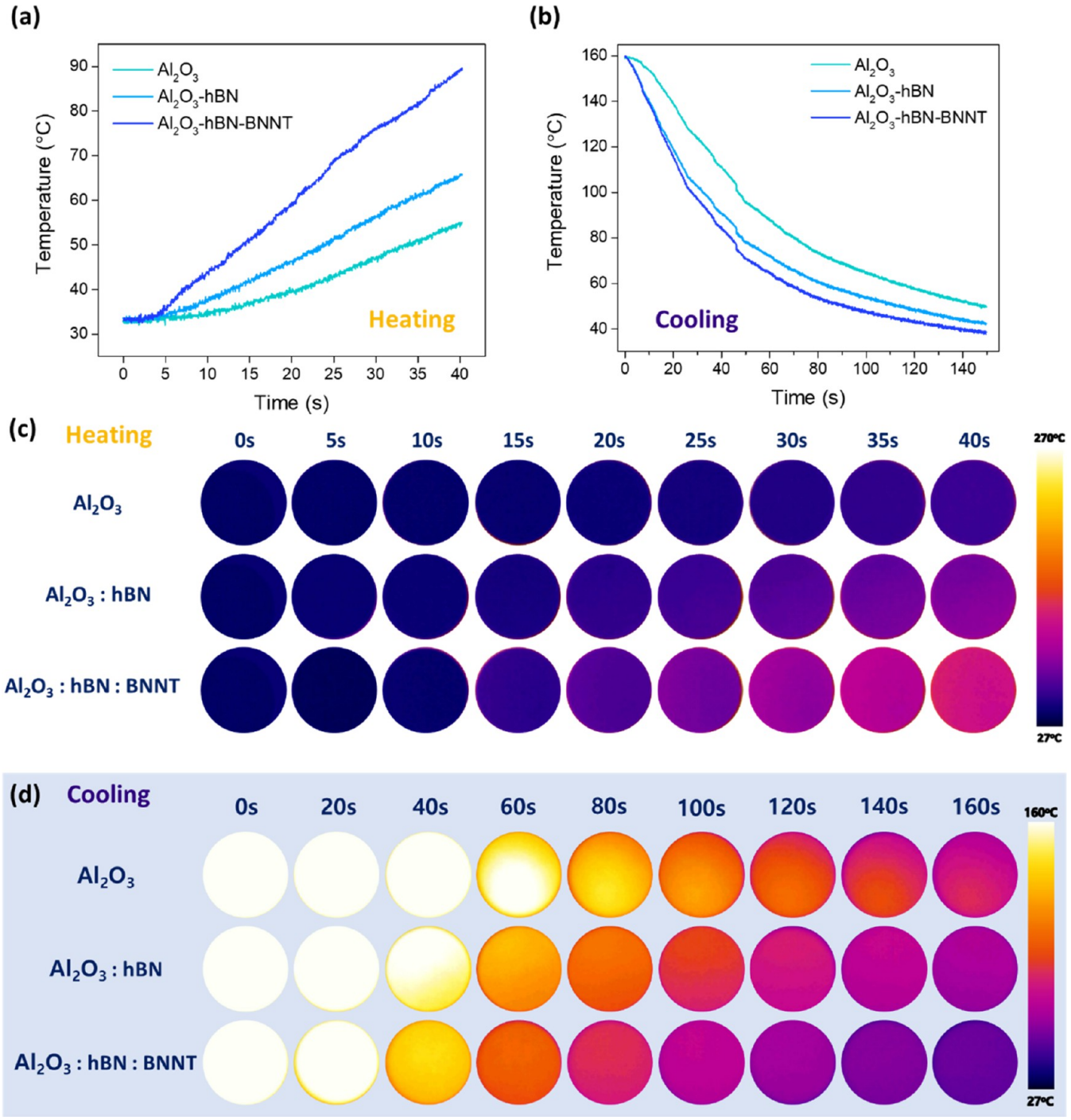

Figure 8. (a) Heating and (b) cooling propagation of unary, secondary, and ternary filler composites and (c, d) their corresponding thermal infrared images.

fractions of h-BN and BNNT were explored to accentuate and analyze their contribution to the conductive pathway formation and thermal transport performance. In the composite preparation, the amount of Al_2O_3 particles was maintained at 76.5 wt % while varying the ratio of h-BN and BNNT, where the fraction of the boron nitride derivatives was maintained at 13.5 wt %. As shown in Figure 7b, variation in thermal conductivity was also observed with respect to the changes in the filler additive ratios. The thermal performances of the bimodal systems with h-BN/BNNT ratios of ~1:0 (only h-BN) and ~0:1 (only BNNT) were compared with those of the ternary systems. Al_2O_3-BNNT demonstrated a much higher thermal conductivity than Al_2O_3-h-BN, while the introduction of BNNT with an h-BN/BNNT ratio of ~ 2:1 presents the highest isotropic thermal conductivity of 7.50 W/mK, which increases ~50% relative to the Al_2O_3/h-BN binary filler composite. It should be noted that the thermal conductivity with other ratios decreased as BNNT content increased; this might be due to severe aggregation of BNNT, resulting in inhomogeneous dispersion and lower thermal conductivity, possibly due to the lack of heat conduction pathways in the composite. However, much higher heat

https://doi.org/10.1021/acsomega.3c02246
ACS Omega 2023, 8, 24454−24466

dissipation performance can be expected, as the BNNT fraction increases if the homogeneous dispersion is attained. Overall, it can be claimed that the ternary network posted a good technique for modifying the bulk thermal conductivity, since all of the ternary samples show a higher thermal induction performance in comparison with their bimodal counterparts.

3.4. Practical Thermal Management Performance. As 5G makes its way toward our smart devices, a distinct dilemma emerges with it; with the higher performance demand translated to densified devices, the occurrence of a thermal heating problem is no surprise.[28] Consequently, to exhibit the feasibility of the fabricated composite for thermal management applications, we devised a heating apparatus that imitate the heating amplitude of microchips on electronic devices, as illustrated in Figure S5. The heating and cooling propagation of the prepared composites is illustrated in Figure 8a−d, and all samples follow an increasing profile upon heat exposure. It can be discerned that the ternary filler composite demonstrated the highest thermal dissipation performance analogous to the thermal conductivity performance, which can be associated with the establishment of a continuous filler network. This demonstrates the efficacy of the structured framework mitigation on heat dissipation augmentation.[47] Owing to its high thermal conductivity, the ternary filler composite exhibited higher interfacial thermal increase propagation, as it reached 89.67 °C after 40 s, while the binary and unary composites reached roughly 65.86 and 55.27 °C, respectively, at the same time. In addition, the interfacial temperature of the ternary composite was about ∼36.15 and ∼62.24% higher than its binary and unary composite counterparts, respectively, indicating the enhancement of the phonon transfer network due to the assimilation of BNNT. Moreover, the ternary filler composite displayed a uniform heating distribution on its surface compared to its corresponding derivatives, which can be realized from the heating gradient occurrence onto the interface of the composite upon heat exposure, indicating its dominant isotropic attribute. The cooling proliferation follows the trend, as the heating profile with the ternary filler system obtains the accelerated cooling response.

3.5. Thermal Conductivity Properties and Mechanism. Considering the heat dissipation paradigm of the developed ternary composite, which can be constituted by the spatial and orientational filler modifications influenced by how the compounding fillers intercalated with each other, a computational evaluation was accomplished to precisely construe the thermal conductivity, interfacial thermal resistance (ITR), and the heat transport mechanism of the articulated ternary filler composite. To better understand the underlying mechanism governing the thermal conductivity enhancement, two parametric variables were explored using eqs 1 and 2; thermal enhancement factor (ϕ), which depicts the thermal conductivity improvement, and thermal improvement efficiency (η), which represents the thermal conductivity augmentation per 1 vol % loading.[49]

$$\phi = \frac{k_c - k_m}{k_m} \times 100\% \quad (1)$$

where k_c and k_m are the thermal conductivities of the ternary composite and the polymeric matrix, respectively.

$$\eta = \frac{k_c - k_m}{100 W_f k_m} \times 100\% \quad (2)$$

where w_f is the weight fraction of the fillers.

The calculated thermal enhancement factor and thermal enhancement efficiency are depicted in Figure 9a,b. As

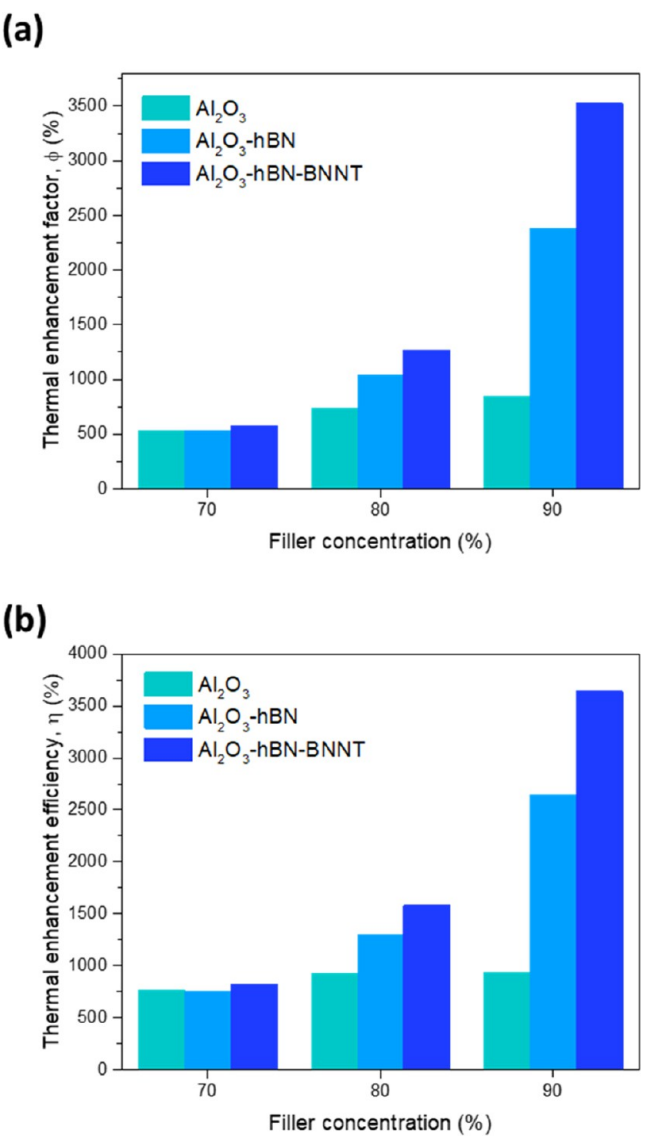

Figure 9. Prepared ternary composite and its derivatives (a, b) with different concentrations and its corresponding thermal conductivity (ϕ) factor and (η) efficiency.

elaborated, k gravely improves upon the assimilation of the ternary filler network, obtaining a maximum thermal enhancement factor of 3650%, which is a 36-fold increase compared to neat PDMS and almost 297% (3-fold) of its primary composite counterpart. Similarly, the thermal improvement efficiency signifies a substantial enhancement in the thermal conductivity performance. These affirm the significant contribution of the postulated ternary filler blend to thermal conductivity, which can be associated with 3D heat conduction pathways from the oriented multidimensional fillers. Because of these conductive paths, phonons can freely flow without internally accumulating on the composite matrix.

https://doi.org/10.1021/acsomega.3c02246
ACS Omega 2023, 8, 24454−24466

To hypothetically assess intrinsic factors influencing thermal conductivity enhancement, the Agari model was employed to evaluate the thermal conductivity of the ternary composite and its subsequent derivatives using eq 3, where V_f is the volume fraction of the filler. In the Agari model, C_1 stands for the index measurement of the influence of the polymeric matrix. Due to the negligible influence of PDMS on the filler's interaction, C_1 can be deemed to be 1, in agreement with the theory. C_2 on the other hand is a parameter pertaining to the ability of the fillers to form a thermally conductive pathway. According to theory, the value of C_2 is commonly between 0 and 1, a higher C_2 value signifies easier construction of continuous heat conduction channels; for the simulated k_c value, C_2 is set as 1.[50] As presented in Figure 10a, the simulated thermal conductivity was marginally lower than the experimental results of the composites. It can be discerned that the predicted thermal conductivity follows the same trend as the experimental thermal conductivity in various modes. Moreover, upon applying the experimental bulk thermal conductivity measurements of the ternary, binary, and primary composites to the Agari model, the conveyed C_2 values were 0.84, 0.74, and 0.62, respectively. It can be realized that the ternary composite acquired the highest C_2 value, highlighting the ability of BNNT to establish transmission phonon passage and thereby reducing the occurrence of phonon scattering.

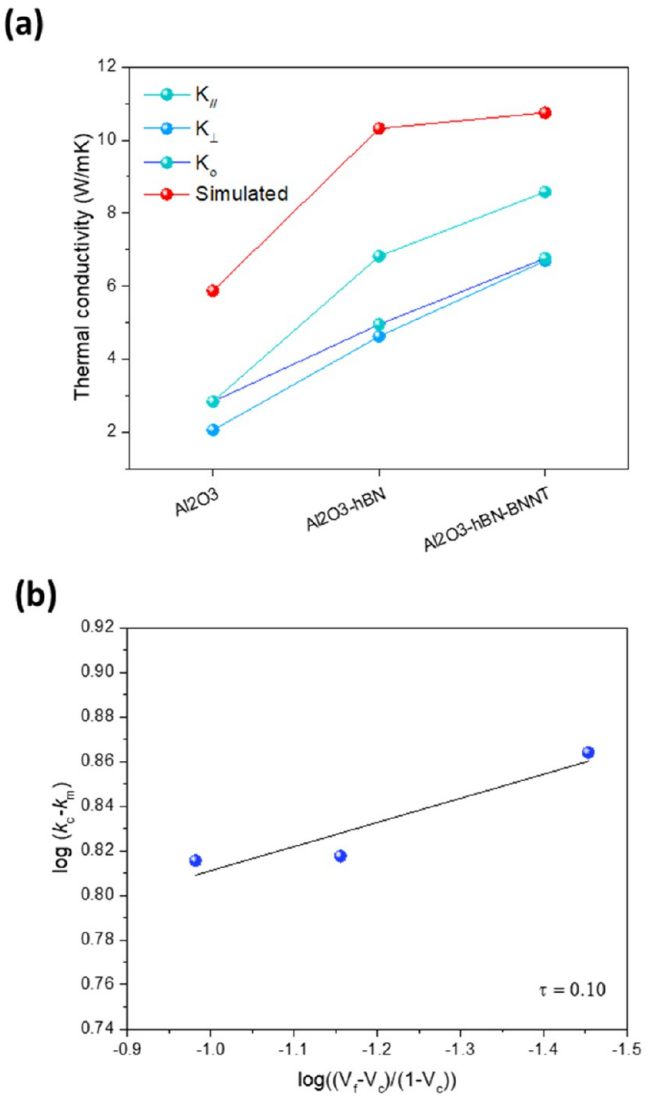

Figure 10. (a) Different thermal conductivities ($k_{//}$, $k_{\perp}$, and k_o) with the simulated Agari model profile. (b) Plotted experimental results based on Foygel's nonlinear model.

$$\log K_c = V_f C_2 \log(K_f) - (1 - V_f) C_1 \log(K_m) \quad (3)$$

To theoretically evaluate the component governing the thermal conductivity improvement from the interfiller point of view, Nan's and Foygel's models were adopted.[38,51,52] Nan's model implemented a strategy that considers the effect of nanotubes on thermal conductivity improvement; the derived equations are presented in the Supporting Information. The obtained ITR value of the ternary composite is 1.28×10^{-9} m^2K/W, which is 1 order of magnitude lower than that of the binary composite (1.34×10^{-8} m^2K/W). These simulated values greatly agree with the measured thermal conductivity, considering the phonon conduction improvement of the bridging effect of BNNT. Hence, Nan's model is not entirely fitting for the ITR estimation of the ternary filler composite, since the model is based on the hypothesis that the filler is completely covered with a polymeric matrix, which is conflicting with the iterated interaction between the multidimensional fillers. Therefore, a nonlinear model proposed by Foygel et al. was adopted as follows[53]

$$k_c - k_m = k_o \left(\frac{V_f - V_c}{1 - V_f} \right)^{\tau} \quad (4)$$

$$R_c = \frac{1}{k_o L V_c^{\tau}} \quad (5)$$

$$R = R_c S \quad (6)$$

where k_o is implied as the preexponential factor ratio of probable interaction of the filler network, τ is the conductivity exponent that relies on the fillers' aspect ratio, V_c is the critical volume fraction of the filler, R_c is the contact resistance between the intercalated fillers, and R_f is the interfacial thermal resistance.[52] The values of k_o (2.08 10^3 W/mK) and τ (0.10) were obtained by fitting the experimental data of the ternary composite into the Foygel equation, as presented in Figure 10b. The calculated R_c of the ternary composite was around 1.26×10^3 K/W; based on this result, the ITR value can be acquired at 5.04×10^{-12} m^2K/W, which is much smaller than the acquired value for binary composite (1.55×10^{-10} m^2K/W). This quantitatively illustrates the contacting enhancement contribution of BNNT, which is in accord with the thermal conductivity performance of the compounded composite.

As discussed, it is stipulated that the integration of multiscale fillers plays a crucial role in thermal conductivity augmentation. The premise of our design is to enhance thermal conductivity through the assimilation of Al_2O_3, h-BN, and BNNT forming 3D interconnected pathways to administer effective phonon transport and reduce phonon scattering, as demonstrated in Figure 11, with h-BN prohibiting the occurrence of hotspots, which can be correlated to its dominant contribution to $k_{//}$. The introduction of BNNT provides a bridging effect for phonon transport and construction of interconnected networks allowing heat dissipation in multiple directions, insinuating isotropic thermal flow, as observed in the thermal conductivity results. This implies the effective interaction between the multidimensional fillers and the formation of a continuous

https://doi.org/10.1021/acsomega.3c02246
ACS Omega 2023, 8, 24454−24466

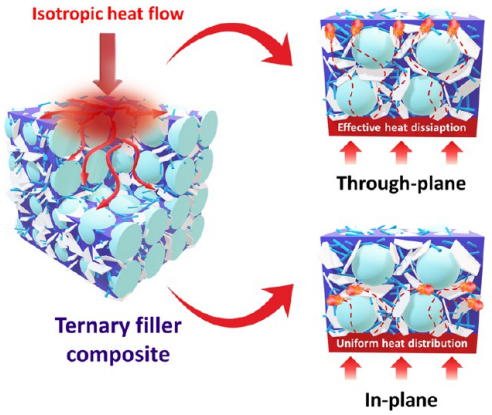

Figure 11. Isotropic heat dissipation mechanism of the crafted ternary filler composite and its corresponding phonon route in vertical and horizontal directions.

cluster for effective phonon transport within the composite matrices. Moreover, due to the identical elemental attribute of h-BN and BNNT, it can be postulated that their assimilation can induce improved phonon conduction due to the phonon-matching acoustic property, thereby promoting seamless phonon transport and reduction of phonon scattering.[31]

3.6. Isotropic Performance. The formation of an oriented filler to form a 3D structure to induce thermal conductivity enhancement had been comprehensively expounded to address the current limitations of TIM composites, particularly the thermal conductivity direction modification, which gravely influences the thermal dissipation attributes. Therefore, to shed light on the parametric requirement of TIM, we thoroughly scrutinized the established techniques addressing these constraints. Presented in Table 2 is the summary of the recent advances in fabrication strategies on directional thermal conductivity modification of boron nitride-based composites. Hence, the majority of this research demonstrated complicated assembly techniques with minimal axial thermal conductivity improvement, which highlights the contribution of this work. The proposed ternary filler framework exhibits ultralow discrepancy between the radial and axial thermal conductivities, obtaining an isotropic ratio of 1.35, which can be accounted for the effective phonon pathway of the articulated ternary filler system. This highly suggests the synergistic interaction and effective percolation arrangement of the ternary filler blend and the bridging effect contribution of BNNT, which minimize the phonon scattering effect, leading to a continuous heat flow.

4. CONCLUSIONS

In the discussed research article, an exceptional strategy to implicate high overall thermal conductivity, adopting a ternary filler design, employed a thorough assimilation of multiscale fillers to enunciate conducting pathways. The suggested ternary filler framework presents reduced discrepancy between the radial and axial thermal conductivities, acquiring an isotropic ratio of 1.35, which can be correlated to the generated continuous phonon pathway of the articulated filler system. Moreover, this strategy facilitated an immense thermal dissipation improvement, obtaining a low isotropic ratio of 1.35 between in-plane and through-plane thermal conductivities while obtaining a maximum isotropic thermal conductance of 7.50 W/mK, which is about a 3650% improvement from pristine PDMS and nearly 3-fold (∼297%) that of the Al_2O_3 unary filler composite and ∼53% from its binary equivalent, contributing interfacial thermal differences of ∼36.15 and ∼62.24% on applied heating performance compared to its counterparts. Henceforth, the assimilation of BNNT in the compounded system provides an advantageous contribution not only to the thermal conductance perspective but also to structural permeance. Enhancement in thermal permanency is postulated due to a melting point (T_m) shift of ∼11 °C upon the integration of BNNT. Mechanical stability fortification was also perceived with the presence of BNNT, incurring a 31.5% escalation in tensile strength and a 53% inclination in Young's modulus relative to the unary filler composite. The presented strategy illustrated an innovative insight into composite engineering. The assimilation of the two derivatives of boron nitride-constituted percolation promotion which opens up a new avenue for the construction and fabrication of TIM for high thermal conductivity performance. Additionally, BNNT also exhibited a relative impact on the thermal and mechanical stability standpoint due to their intrinsic stability and structural flexibility. These results offer new insights into heat conduction phenomena in a polymeric composite system and propose a systematic strategy for the design and construction of industrial TIM.

■ ASSOCIATED CONTENT

Supporting Information

The Supporting Information is available free of charge at https://pubs.acs.org/doi/10.1021/acsomega.3c02246.

SEM images of the primary, secondary, and ternary fillers: (a, b) Al_2O_3, (c, d) h-BN, and (e, f) BNNT (Figure S1); SEM images of the fabricated primary, secondary, and ternary filler systems: (a, b) PDMS-Al_2O_3, (c, d) PDMS-Al_2O_3-h-BN, and (e, f) PDMS-Al_2O_3-h-BN-BNNT (Figure S2); SEM images of the fabricated filler composite with different ratios of h-BN

Table 2. Thermal Conductivity Performance of Boron Nitride-Based Composite

polymer	filler	filler concentration (%)	$k_{//}$	$k_{\perp}$	k_o	isotropic ratio	refs
PVDF	PES/h-BN	42	20.56	2.82	13.13	7.29	49
HDPE	h-BN	20.9	3.21	1.34	2.07	2.39	26
epoxy	BNNS	15	6.07	0.51		12.00	54
PVDF	BNNS	33	16.3	0.78		21.00	27
PVA	h-BN	27	8.44	1.63		5.18	55
VAE resin	PA6/h-BN	21	8.96	1.5		5.97	30
PVA	BNNT	10	0.54	0.18		3.00	56
PDMS	Al_2O_3/h-BN/BNNT	90	7.66	5.656	7.50	1.35	this work

https://doi.org/10.1021/acsomega.3c02246
ACS Omega 2023, 8, 24454−24466

and BNNT (h-BN/BNNT): (a) 2:1, (b) 1:1, and (c) 1:2 (Figure S3); fabricated ternary filler composite (Figure S4); practical thermal dissipation setup (Figure S5); Nans' model employed in the ITR analysis for the ternary composite and its corresponding derivatives; and geometrical correlation applied to the ITR analysis (PDF)

AUTHOR INFORMATION

Corresponding Author

Jaewoo Kim − *R&D Center, Naieel Technology, Daejeon 34104, Republic of Korea;* orcid.org/0000-0003-3472-0180; Email: kimj@naieel.com

Authors

Arni Gesselle M. Pornea − *R&D Center, Naieel Technology, Daejeon 34104, Republic of Korea*

Ki-In Choi − *R&D Center, Naieel Technology, Daejeon 34104, Republic of Korea*

Jung-Hwan Jung − *R&D Center, Naieel Technology, Daejeon 34104, Republic of Korea;* orcid.org/0000-0002-3352-1940

Zahid Hanif − *R&D Center, Naieel Technology, Daejeon 34104, Republic of Korea*

Cheolwoo Kwak − *CMT Co., Ltd., Seoul 06211, Republic of Korea*

Complete contact information is available at: https://pubs.acs.org/10.1021/acsomega.3c02246

Notes

The authors declare no competing financial interest.

ACKNOWLEDGMENTS

This work was financially supported by Project Grant No. S3043060 sponsored by the Ministry of SMEs and Startups and Project Grant No. 20017989 (ATC+ Program) sponsored by the Ministry of Trade, Industry and Energy of the Republic of Korea.

REFERENCES

(1) Singh, S. K.; Sharan, T.; Singh, A. K. Enhancing the Axial Ratio Bandwidth of Circularly Polarized Open Ground Slot CPW-Fed Antenna for Multiband Wireless Communications. *Eng. Sci.* **2021**, *17*, 274−284.

(2) Al-Zhrani, S.; Bedaiwi, N. M.; El-Ramli, I. F.; Barasheed, A. Z.; Abduldaiem, A.; Al-Hadeethi, Y.; Umar, A. Underwater Optical Communications: A Brief Overview and Recent Developments. *Eng. Sci.* **2021**, *16*, 146−186.

(3) Xu, J.; Cao, J.; Guo, M.; Yang, S.; Yao, H.; Lei, M.; Hao, Y.; Bi, K. Metamaterial Mechanical Antenna for Very Low Frequency Wireless Communication. *Adv. Compos. Hybrid Mater.* **2021**, *4*, 761−767.

(4) Cao, J.; Yao, H.; Pang, Y.; Xu, J.; Lan, C.; Lei, M.; Bi, K. Dual-Band Piezoelectric Artificial Structure for Very Low Frequency Mechanical Antenna. *Adv. Compos. Hybrid Mater.* **2022**, *5*, 410−418.

(5) Xu, X.; Chen, J.; Zhou, J.; Li, B. Thermal Conductivity of Polymers and Their Nanocomposites. *Adv. Mater.* **2018**, *30*, No. 1705544.

(6) Hansson, J.; Nilsson, T. M. J.; Ye, L.; Liu, J. Novel Nanostructured Thermal Interface Materials: A Review. *Int. Mater. Rev.* **2018**, *63*, 22−45.

(7) Song, N.; Jiao, D.; Cui, S.; Hou, X.; Ding, P.; Shi, L. Highly Anisotropic Thermal Conductivity of Layer-by-Layer Assembled Nanofibrillated Cellulose/Graphene Nanosheets Hybrid Films for Thermal Management. *ACS Appl. Mater. Interfaces* **2017**, *9*, 2924−2932.

(8) Lei, L.; Bolzoni, L.; Yang, F. Interphase Layer Characteristics and Thermal Conductivity of Hot-Forged Cu-B/Diamond Composites. *Adv. Compos. Hybrid Mater.* **2022**, *5*, 1527−1536.

(9) Hu, X.; Wu, H.; Lu, X.; Liu, S.; Qu, J. Improving Thermal Conductivity of Ethylene Propylene Diene Monomer/Paraffin/Expanded Graphite Shape-Stabilized Phase Change Materials with Great Thermal Management Potential via Green Steam Explosion. *Adv. Compos. Hybrid Mater.* **2021**, *4*, 478−491.

(10) Xie, Y.; Yang, Y.; Liu, Y.; Wang, S.; Guo, X.; Wang, H.; Cao, D. Paraffin/Polyethylene/Graphite Composite Phase Change Materials with Enhanced Thermal Conductivity and Leakage-Proof. *Adv. Compos. Hybrid Mater.* **2021**, *4*, 543−551.

(11) Pan, D.; Dong, J.; Yang, G.; Su, F.; Chang, B.; Liu, C.; Zhu, Y.-C.; Guo, Z. Ice Template Method Assists in Obtaining Carbonized Cellulose/Boron Nitride Aerogel with 3D Spatial Network Structure to Enhance the Thermal Conductivity and Flame Retardancy of Epoxy-Based Composites. *Adv. Compos. Hybrid Mater.* **2022**, *5*, 58−70.

(12) Zhang, H.; Zhang, X.; Li, D.; Zhuang, J.; Liu, Y.; Liu, H.; Wu, D.; Feng, J.; Sun, J. Synergistic Enhanced Thermal Conductivity of Polydimethylsiloxane Composites via Introducing SCF and Hetero-Structured GB@rGO Hybrid Fillers. *Adv. Compos. Hybrid Mater.* **2022**, *5*, 1756−1768.

(13) Jing, X.; Li, Y.; Zhu, J.; Chang, L.; Maganti, S.; Naik, N.; Xu, B. B.; Murugadoss, V.; Huang, M.; Guo, Z. Improving Thermal Conductivity of Polyethylene/Polypropylene by Styrene-Ethylene-Propylene-Styrene Wrapping Hexagonal Boron Nitride at the Phase Interface. *Adv. Compos. Hybrid Mater.* **2022**, *5*, 1090−1099.

(14) Zeng, X.; Yao, Y.; Gong, Z.; Wang, F.; Sun, R.; Xu, J.; Wong, C. P. Ice-Templated Assembly Strategy to Construct 3D Boron Nitride Nanosheet Networks in Polymer Composites for Thermal Conductivity Improvement. *Small* **2015**, *11*, 6205−6213.

(15) Chen, H.; Ginzburg, V. V.; Yang, J.; Yang, Y.; Liu, W.; Huang, Y.; Du, L.; Chen, B. Thermal Conductivity of Polymer-Based Composites: Fundamentals and Applications. *Prog. Polym. Sci.* **2016**, *59*, 41−85.

(16) Zhi, C. Y.; Bando, Y.; Wang, W. L.; Tang, C. C.; Kuwahara, H.; Golberg, D. Mechanical and Thermal Properties of Polymethyl Methacrylate-BN Nanotube Composites. *J. Nanomater.* **2008**, *2008*, 1−5.

(17) Chen, J.; Huang, X.; Zhu, Y.; Jiang, P. Cellulose Nanofiber Supported 3D Interconnected BN Nanosheets for Epoxy Nanocomposites with Ultrahigh Thermal Management Capability. *Adv. Funct. Mater.* **2017**, *27*, No. 1604754.

(18) Jung, J.; Kim, J.; Uhm, Y. R.; Jeon, J. K.; Lee, S.; Lee, H. M.; Rhee, C. K. Preparations and Thermal Properties of Micro- and Nano-BN Dispersed HDPE Composites. *Thermochim. Acta* **2010**, *499*, 8−14.

(19) Zhang, K.; Ma, Z.; Deng, H.; Fu, Q. Improving High-Temperature Energy Storage Performance of PI Dielectric Capacitor Films through Boron Nitride Interlayer. *Adv. Compos. Hybrid Mater.* **2022**, *5*, 238−249.

(20) Clausi, M.; Zahid, M.; Shayganpour, A.; Bayer, I. S. Polyimide Foam Composites with Nano-Boron Nitride (BN) and Silicon Carbide (SiC) for Latent Heat Storage. *Adv. Compos. Hybrid Mater.* **2022**, *5*, 798−812.

(21) Hu, D.; Liu, H.; Yang, M.; Guo, Y.; Ma, W. Construction of Boron Nitride Nanosheets-Based Nanohybrids by Electrostatic Self-Assembly for Highly Thermally Conductive Composites. *Adv. Compos. Hybrid Mater.* **2022**, *5*, 3201−3211.

(22) Zhang, W.; Feng, Y.; Althakafy, J. T.; Liu, Y.; Abo-Dief, H. M.; Huang, M.; Zhou, L.; Su, F.; Liu, C.; Shen, C. Ultrahigh Molecular Weight Polyethylene Fiber/Boron Nitride Composites with High Neutron Shielding Efficiency and Mechanical Performance. *Adv. Compos. Hybrid Mater.* **2022**, *5*, 2012−2020.

(23) Li, M.; Wang, M.; Hou, X.; Zhan, Z.; Wang, H.; Fu, H.; Lin, C.-T.; Fu, L.; Jiang, N.; Yu, J. Highly Thermal Conductive and Electrical

Insulating Polymer Composites with Boron Nitride. *Composites, Part B* **2020**, *184*, No. 107746.
(24) Hu, J.; Huang, Y.; Yao, Y.; Pan, G.; Sun, J.; Zeng, X.; Sun, R.; Xu, J.-B.; Song, B.; Wong, C.-P. Polymer Composite with Improved Thermal Conductivity by Constructing a Hierarchically Ordered Three-Dimensional Interconnected Network of BN. *ACS Appl. Mater. Interfaces* **2017**, *9*, 13544−13553.
(25) Zhou, W.; Zhang, Y.; Wang, J.; Li, H.; Xu, W.; Li, B.; Chen, L.; Wang, Q. Lightweight Porous Polystyrene with High Thermal Conductivity by Constructing 3D Interconnected Network of Boron Nitride Nanosheets. *ACS Appl. Mater. Interfaces* **2020**, *12*, 46767−46778.
(26) Hamidinejad, M.; Zandieh, A.; Lee, J. H.; Papillon, J.; Zhao, B.; Moghimian, N.; Maire, E.; Filleter, T.; Park, C. B. Insight into the Directional Thermal Transport of Hexagonal Boron Nitride Composites. *ACS Appl. Mater. Interfaces* **2019**, *11*, 41726−41735.
(27) Chen, J.; Huang, X.; Sun, B.; Jiang, P. Highly Thermally Conductive Yet Electrically Insulating Polymer/Boron Nitride Nanosheets Nanocomposite Films for Improved Thermal Management Capability. *ACS Nano* **2019**, *13*, 337−345.
(28) Chen, J.; Huang, X.; Sun, B.; Wang, Y.; Zhu, Y.; Jiang, P. Vertically Aligned and Interconnected Boron Nitride Nanosheets for Advanced Flexible Nanocomposite Thermal Interface Materials. *ACS Appl. Mater. Interfaces* **2017**, *9*, 30909−30917.
(29) Chen, J.; Wei, H.; Bao, H.; Jiang, P.; Huang, X. Millefeuille-Inspired Thermally Conductive Polymer Nanocomposites with Overlapping BN Nanosheets for Thermal Management Applications. *ACS Appl. Mater. Interfaces* **2019**, *11*, 31402−31410.
(30) Zhang, X.; Wu, K.; Liu, Y.; Yu, B.; Zhang, Q.; Chen, F.; Fu, Q. Preparation of Highly Thermally Conductive but Electrically Insulating Composites by Constructing a Segregated Double Network in Polymer Composites. *Compos. Sci. Technol.* **2019**, *175*, 135−142.
(31) Yao, Y.; Sun, J.; Zeng, X.; Sun, R.; Xu, J.-B.; Wong, C.-P. Construction of 3D Skeleton for Polymer Composites Achieving a High Thermal Conductivity. *Small* **2018**, *14*, No. 1704044.
(32) Wang, D.; Wei, H.; Lin, Y.; Jiang, P.; Bao, H.; Huang, X. Achieving Ultrahigh Thermal Conductivity in Ag/MXene/Epoxy Nanocomposites via Filler-Filler Interface Engineering. *Compos. Sci. Technol.* **2021**, *213*, No. 108953.
(33) Wu, K.; Fang, J.; Ma, J.; Huang, R.; Chai, S.; Chen, F.; Fu, Q. Achieving a Collapsible, Strong, and Highly Thermally Conductive Film Based on Oriented Functionalized Boron Nitride Nanosheets and Cellulose Nanofiber. *ACS Appl. Mater. Interfaces* **2017**, *9*, 30035−30045.
(34) Jiang, N.; Hu, D.; Xu, Y.; Chen, J.; Chang, X.; Zhu, Y.; Li, Y.; Guo, Z. Ionic Liquid Enabled Flexible Transparent Polydimethylsiloxane Sensors for Both Strain and Temperature Sensing. *Adv. Compos. Hybrid Mater.* **2021**, *4*, 574−583.
(35) Wu, H.; Sun, H.; Han, F.; Xie, P.; Zhong, Y.; Quan, B.; Zhao, Y.; Liu, C.; Fan, R.; Guo, Z. Negative Permittivity Behavior in Flexible Carbon Nanofibers-Polydimethylsiloxane Films. *Eng. Sci.* **2022**, *17*, 113−120.
(36) Hanif, Z.; Choi, K. I.; Jung, J. H.; Pornea, A. G. M.; Park, E.; Cha, J.; Kim, H. R.; Choi, J. H.; Kim, J. Dispersion Enhancement of Boron Nitride Nanotubes in a Wide Range of Solvents Using Plant Polyphenol-Based Surface Modification. *Ind. Eng. Chem. Res.* **2022**, *62*, 2662−2670.
(37) Li, Y.-T.; Liu, W.-J.; Shen, F.-X.; Zhang, G.-D.; Gong, L.-X.; Zhao, L.; Song, P.; Gao, J.-F.; Tang, L.-C. Processing, Thermal Conductivity and Flame Retardant Properties of Silicone Rubber Filled with Different Geometries of Thermally Conductive Fillers: A Comparative Study. *Composites, Part B* **2022**, *238*, No. 109907.
(38) Zeng, X.; Sun, J.; Yao, Y.; Sun, R.; Xu, J.-B.; Wong, C.-P. A Combination of Boron Nitride Nanotubes and Cellulose Nanofibers for the Preparation of a Nanocomposite with High Thermal Conductivity. *ACS Nano* **2017**, *11*, 5167−5178.
(39) Yanar, N.; Yang, E.; Park, H.; Son, M.; Choi, H. Boron Nitride Nanotube (BNNT) Membranes for Energy and Environmental Applications. *Membranes* **2020**, *10*, No. 430.
(40) Li, X.; Li, Y.; Alam, M. M.; Miao, J.; Chen, P.; Xia, R.; Wu, B.; Qian, J. Enhanced Through-Plane Thermal Conductivity in Polymer Nanocomposites by Constructing Graphene-Supported BN Nanotubes. *J. Mater. Chem. C* **2020**, *8*, 9569−9575.
(41) Razeeb, K. M.; Dalton, E.; Cross, G. L. W.; Robinson, A. J. Present and Future Thermal Interface Materials for Electronic Devices. *Int. Mater. Rev.* **2018**, *63*, 1−21.
(42) Pornea, A. G. M.; Puguan, J. M. C.; Ruello, J. L. A.; Kim, H. Multifunctional Dual-Pore Network Aerogel Composite Material for Broadband Sound Absorption, Thermal Insulation, and Fire Repellent Applications. *ACS Appl. Polym. Mater.* **2022**, *4*, 2880−2895.
(43) Cui, X.; Zhu, G.; Pan, Y.; Shao, Q.; Zhao, C.; Dong, M.; Zhang, Y.; Guo, Z. Polydimethylsiloxane-Titania Nanocomposite Coating: Fabrication and Corrosion Resistance. *Polymer* **2018**, *138*, 203−210.
(44) Liu, D.; Ma, C.; Chi, H.; Li, S.; Zhang, P.; Dai, P. Enhancing Thermal Conductivity of Polyimide Composite Film by Electrostatic Self-Assembly and Two-Step Synergism of Al 2 O 3 Microspheres and BN Nanosheets. *RSC Adv.* **2020**, *10*, 42584−42595.
(45) Hassan, J.; Ikram, M.; Ul-Hamid, A.; Imran, M.; Aqeel, M.; Ali, S. Application of Chemically Exfoliated Boron Nitride Nanosheets Doped with Co to Remove Organic Pollutants Rapidly from Textile Water. *Nanoscale Res. Lett.* **2020**, *15*, No. 75.
(46) Chang, T.-C.; Liao, C.-A.; Lin, Z.-Y.; Fuh, Y.-K. Highly Stretchable Thermal Interface Materials with Uniformly Dispersed Network of Exfoliated Graphite Nanoplatelets via Ball Milled Processing Route. *Microsyst. Technol.* **2018**, *24*, 3667−3675.
(47) Liu, B.; Li, Y.; Fei, T.; Han, S.; Xia, C.; Shan, Z.; Jiang, J. Highly Thermally Conductive Polystyrene/Polypropylene/Boron Nitride Composites with 3D Segregated Structure Prepared by Solution-Mixing and Hot-Pressing Method. *Chem. Eng. J.* **2020**, *385*, No. 123829.
(48) Dong, M.; Zhang, H.; Tzounis, L.; Santagiuliana, G.; Bilotti, E.; Papageorgiou, D. G. Multifunctional Epoxy Nanocomposites Reinforced by Two-Dimensional Materials: A Review. *Carbon* **2021**, *185*, 57−81.
(49) Gao, Y.; Zhang, M.; Chen, X.; Zhu, Y.; Wang, H.; Yuan, S.; Xu, F.; Cui, Y.; Bao, D.; Shen, X.; Sun, Y.; Peng, J.; Zhou, Y.; Zhang, M. A High-Performance Thermal Conductive and Outstanding Electrical Insulating Composite Based on Robust Neuron-like Microstructure. *Chem. Eng. J.* **2021**, *426*, No. 131280.
(50) Agari, Y.; Uno, T. Estimation on Thermal Conductivities of Filled Polymers. *J. Appl. Polym. Sci.* **1986**, *32*, 5705−5712.
(51) Nan, C.-W.; Liu, G.; Lin, Y.; Li, M. Interface Effect on Thermal Conductivity of Carbon Nanotube Composites. *Appl. Phys. Lett.* **2004**, *85*, 3549−3551.
(52) Wang, S.; Li, W.; Jin, X.; Wu, J.; Chen, K.; Gan, W. Facile Fabrication of Three-Dimensional Thermal Conductive Composites with Synergistic Effect of Multidimensional Fillers. *J. Mater. Sci.* **2021**, *56*, 12671−12685.
(53) Foygel, M.; Morris, R. D.; Anez, D.; French, S.; Sobolev, V. L. Theoretical and Computational Studies of Carbon Nanotube Composites and Suspensions: Electrical and Thermal Conductivity. *Phys. Rev. B* **2005**, *71*, No. 104201.
(54) Han, J.; Du, G.; Gao, W.; Bai, H. An Anisotropically High Thermal Conductive Boron Nitride/Epoxy Composite Based on Nacre-Mimetic 3D Network. *Adv. Funct. Mater.* **2019**, *29*, No. 1900412.
(55) Zhang, J.; Wang, X.; Yu, C.; Li, Q.; Li, Z.; Li, C.; Lu, H.; Zhang, Q.; Zhao, J.; Hu, M.; Yao, Y. A Facile Method to Prepare Flexible Boron Nitride/Poly(Vinyl Alcohol) Composites with Enhanced Thermal Conductivity. *Compos. Sci. Technol.* **2017**, *149*, 41−47.
(56) Terao, T.; Zhi, C.; Bando, Y.; Mitome, M.; Tang, C.; Golberg, D. Alignment of Boron Nitride Nanotubes in Polymeric Composite Films for Thermal Conductivity Improvement. *J. Phys. Chem. C* **2010**, *114*, 4340−4344.

https://doi.org/10.1021/acsomega.3c02246
ACS Omega 2023, 8, 24454−24466